New mechanistic insights into osmium-based tamoxifen derivatives

Hui Zhi Shirley Lee,[d] François Chau,[a, b] Siden Top,[c] Gérard Jaouen,[c, d] Anne Vessières,[c] Eric Labbé,[a] Olivier Buriez[a*]

[a] PASTEUR, Département de chimie, École normale supérieure, PSL University, Sorbonne Université, CNRS, 75005 Paris, France

[b] Université Paris Diderot, Sorbonne Paris Cité, ITODYS CNRS UMR 7086, 15 rue Jean-Antoine de Baïf, 75205 Paris Cedex 13, France

[c] Sorbonne Université, CNRS, IPCM, 4 Place Jussieu, 75005 Paris, France.

[d] Chimie ParisTech, PSL University, 11 rue Pierre et Marie Curie, 75005 Paris, France

Abstract.

The electrochemical behavior of osmociphenol (**3**, Oc-OH), an organometallic osmium-based anticancer drug candidate, has been investigated by cyclic voltammetry in the absence and presence of lutidine used as a base model. Osmociphenol exhibited spontaneous deprotonation of the phenol function upon oxidation of the osmocene moiety due to its high acidity. In the presence of lutidine, a base-dependent and different electrochemical behavior was observed at low scan rates indicating a second oxidation step leading to the corresponding cationic quinone methide precursor (**3b**$^+$). However, compared to ruthenocene derivatives, the stability of **3b**$^+$ prevented its conversion into quinone methide as the final and stable complex. Despite differences in their oxidative processes, osmociphenol and ruthenociphenol derivatives exhibit similar biological activities.

Keywords. Bioorganometallic; Cyclic voltammetry; Osmium; Anti-Cancer; Tamoxifen

1. Introduction.

Recently, there has been a growing demand for organometallic complexes in the development of innovative anticancer therapies [1-6]. Indeed, organometallic compounds combine as many properties as structural diversity, variable redox states of metals, high lipophilicity and metal-specific reactivity. In this field, recent major contributions have focused on the functionalization of clinically validated purely organic drugs with complexes modified by a metallocene group which exalts the anti-cancer properties of the organic moiety. For instance, grafting a ferrocenyl unit onto chloroquine allowed the preparation of a new molecule called "ferroquine" which possesses a high antiplasmodial activity against the chloroquine resistant FcB1 strain of *Plasmodium falciparum* [7]. Similarly, "ferrocifens" are complexes possessing both a ferrocenyl group and a tamoxifen skeleton, i.e. the current gold standard for endocrine breast cancer therapy [8–10]. The functionalization chemistry achieved on ferrocifens has not only brought more and more efficient molecules [9], but has also contributed to establish a coherent framework for the oxidative metabolism of these compounds [12–16]. The replacement of the ferrocene group by a ruthenocene was recently reported to be of interest for anti-cancer activity [17–19]. More recently, several original osmocene-based tamoxifen derivatives have also been prepared and tested in-vitro against breast cancer cells [20-22]. Interestingly, osmocifen derivatives exhibit similar biological activity than ruthenocifen analogs against MDA-MB231 a hormone-independent breast-cancer cell line (IC_{50}: 34 and 29.7 µM for the ruthenociphenol and osmociphenol derivatives, respectively. See Table 1) [8, 20]. Yet, this does not mean that the oxidative metabolism of both derivatives is the same. On the basis of our electrochemical investigations performed on both ferrocifens and ruthenocifens, the oxidative metabolism of osmocifen complexes is expected to be rooted on the osmocene/ osmocenium (Oc/Oc^+) electron transfer. The mechanism of osmocene electrochemical oxidation has been far less investigated than ferrocifens [20]. In this context, we recently investigated the electrochemical oxidation of osmocene in dichloromethane (DCM) and acetonitrile (MeCN) in the presence of various electrolyte anions ($[BF_4]^-$, $[PF_6]^-$, and $[B(C_6F_5)_4]^-$ (TFAB)) [23]. The preliminary results showed that the reactivity of the electrogenerated osmocenium cation was dramatically affected by the coordinating properties of the electrolyte anion and the donor strength of the solvent.

In the course of our investigation of the reactive sequence of metallocifen drugs, we decided to explore the base-dependent electrochemical behavior of osmociphenol **3** (Scheme 1) in a model environment, i.e. in the presence of a base having a pKa value close to those of peptidic moiety in cells. On the contrary to what was done in the ferrocifen and ruthenocifen series, pyridine could not be used since its nucleophilic character prevails with osmocenium. Instead, the reactivity of the oxidized form of **3** was investigated in the presence of sterically hindered 2,6-lutidine. Under basic conditions, the quinone methide (the final stable complex obtained with ferrocifens) was not formed [24]. Since the anti-cancer properties of ferrocifens were mostly ascribed to this stable oxidized metabolite, we had to revisit the oxidative sequence of osmocifens to explain their anti-proliferative properties.

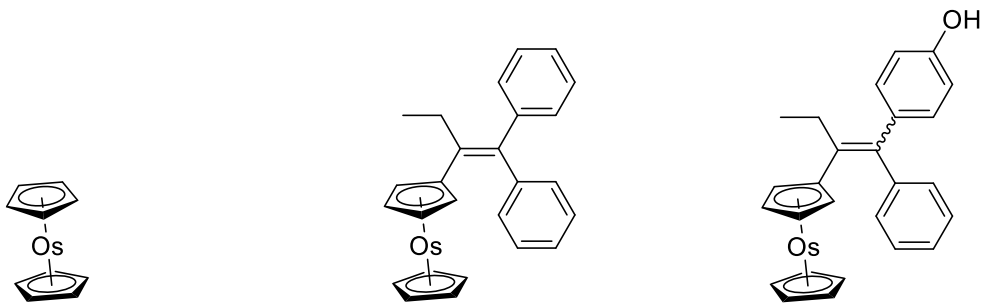

1 **2** **3**

Scheme1. Chemical Structures of osmocene, osmocifen, and osmociphenol derivatives investigated in this work.

Table1. Summary of the oxidation pathways for **3** (Oc-OH) and the corresponding Ru and Fe derivatives.

Compound	IC_{50} (μM) MDA-MB231	Electrochemical oxidation	Enzymatic oxidation; HRP/H_2O_2	Chemical oxidation (Ag_2O)
Oc-OH	34 [20]	- 2 e^- / -1 H	- 2 e^- / -1 H [21]	- 2 e^- / -2 H [20]
Rc-OH	29.7 [20]	- 2 e^- / -2 H [19]	*nd*	- 2 e^- / -2 H [20]
Fc-OH	1.5 [8]	- 2 e^- / -2 H [16]	- 2 e^- / -2 H [36]	- 2 e^- / -2 H [16]

2. Experimental

2.1. Chemicals

Solvents were purchased from Acros Chemicals and used without further purification. Bis(cyclopentadienyl)osmium (Osmocene) was from Strem Chemicals and lithium tetrakis(pentafluorophenyl)borate was from TCI Chemicals; all other chemicals were purchased from other commercial sources (Sigma-Aldrich and Acros) and used as supplied.
Tetrabutylammonium tetrakis(pentafluorophenyl)borate [*n*-Bu_4N][$B(C_6F_5)_4$] ([TBA][TFAB]) was prepared as previously described [23] according to the procedure reported by W.E. Geiger [25].

2.2. Cyclic voltammetry

Cyclic voltammetry measurements were performed by using an Autolab potentiostat (PGSTAT 20). they were carried out at room temperature under an argon atmosphere in a three-electrode cell. The reference electrode was an SCE (saturated calomel electrode; Radiometer), which was separated from the solution by a bridge compartment filled with the same solvent/supporting electrolyte solution as used in the cell. The counter electrode was a platinum wire (1 cm length, Goodfellow). The glass-sealed platinum working electrode disk (0.5 mm diameter, Goodfellow) was homemade. The reproducibility of electrochemical measurements was ensured by careful polishing of the working electrode before each run. Note that in the SCE reference scale the Fc/Fc^+ electrochemical wave is observed at $E_{1/2}$ = 0.40 V vs SCE.

2.3. Synthesis of 1,1-Diphenyl-2-osmocenyl-but-1-ene **2**

$TiCl_4$ (0.20 ml, 1.82 mmol) was added to a suspension of zinc powder (238 mg, 3.64 mmol) in THF (7 ml). The mixture was then heated at reflux for 1 h. A second solution was prepared by dissolving benzophenone (97 mg, 0.52 mmol) and propionyl osmocene (100 mg, 0.26 mmol) in THF (2 ml). This latter solution was added to the first solution and the resulting mixture was heated for 2 hours. After cooling to room temperature, the mixture was hydrolyzed with water (40 ml). After extraction with dichloromethane and solvent removal, the crude product was purified by column chromatography. Hexane/diethyl ether (99/1, v/v) was first used as eluent and after with Hexane/diethyl ether (98/2, v/v). 50 mg of compound was isolated (42 % yield, mp 148°C). ^{1}H NMR (300 MHz, $CDCl_3$) δ: 0.90 (t, 3H, *J* = 7 Hz, CH_3), 2.15 (q, 2H, *J* = 7 Hz, CH_2), 4.40 (t, 1H, *J* = 1.5 Hz, C_5H_4), 4.50 (t, 1H, *J* = 1.5 Hz, C_5H_4), 4.62 (s, 5H, C_5H_5), 7.01-7.24 (m, 10H, 2 C_6H_5). ^{13}C NMR (75.47 MHz, $CDCl_3$) δ: 15.6 (CH_3), 29.7 (CH_2), 63.5 (2CH, C_5H_4), 64.9 (5CH, C_5H_5), 66.0 (2CH, C_5H_4), 126.1 (CH) + 126.2 (CH) + 127.9 (2CH) + 128.1 (2CH) + 129.2 (2CH) + 129.9 (2CH) + 136.9 (C) + 137.8 (C) + 144.2 (C) + 144.3 (C) (2 C_6H_5 + C=C). MS-EI: 529.2 $[M+H]^{\cdot+}$ HRMS (ESI, C26H24OsH: $[M + H]^+$) calcd 529.1566, found 529.1564.

2.4. Synthesis of 1-(4-Hydroxyphenyl)-1-phenyl-2-osmocenyl-but-1-ene (*Z*)- and (*E*)-**3** (Oc-OH)

Osmocifen **3** was synthesized according to a reported process [20] based on the McMurry cross-coupling reaction, as was first reported for the ferrocifen series [26, 27].

3. Results and Discussion.

3.1. Lutidine vs. pyridine as a base model

Recently, we showed that the stability of the electrogenerated osmocenium cation $\mathbf{1}^+$ was dramatically affected by the coordinating properties of the electrolyte anion and/or the donor strength of the solvent [23]. The cyclic voltammogram of **1** obtained in acetonitrile or in the presence of $[BF_4]^-$ as the supporting electrolyte anion, led to irreversible oxidation waves in both cases (Figure 1). Conversely, in dichloromethane (DCM), a low-donor solvent and in the presence of $[B(C_6F_5)_4]^-$ (=[TFAB]) a weakly coordinating supporting electrolyte anion, $\mathbf{1}^+$ was stable on the cyclic voltammetry timescale in agreement with a full reversible wave (Figure 1A, blue curve). Accordingly, we decided to investigate the reactivity of osmium-based tamoxifen derivatives (= "osmocifens") in the same solvent/electrolyte couple, i.e. DCM/[TBA][TFAB].

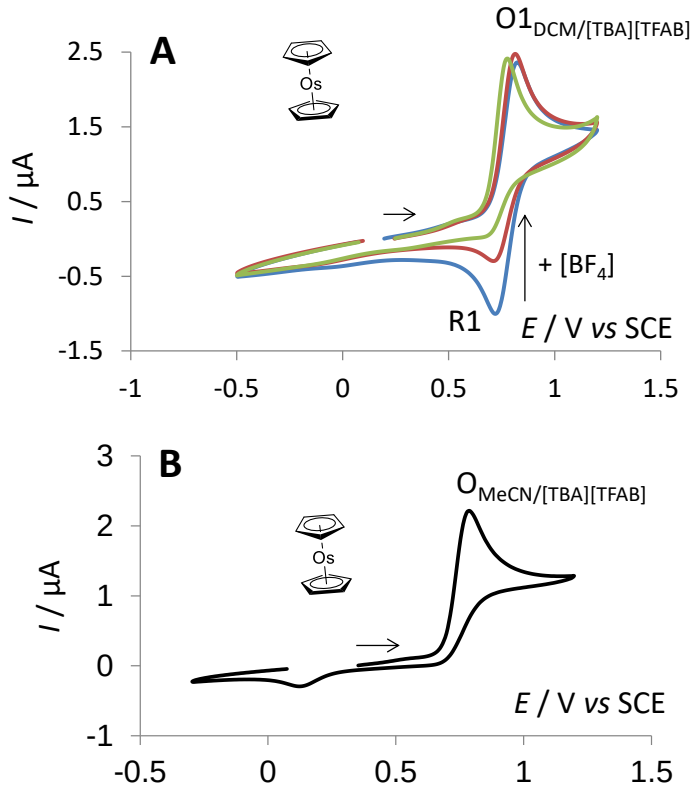

Fig. 1. (A) Cyclic voltammograms of Cp_2Os (**1**, 2 mM), in DCM/[TBA][TFAB] (0.1M), in the absence (blue curve) and in the presence of increasing amounts of $[TBA][BF_4]$ (0.01 M (red curve) and 0.1 M (green curve) respectively). (B) Cyclic voltammogram of Cp_2Os (2 mM), in CH_3CN/[TBA][TFAB] (0.1M). Conditions: studies performed at a Pt electrode, 0.5 mm in diameter; scan rate 200 mV/s. Adapted from [23].

So far, mechanistic investigations involving ferrocene-based tamoxifen derivatives (= "ferrocifens") were performed in the presence of pyridine as base model. Unfortunately, pyridine could not be used to investigate osmocifens due to its nucleophilicity towards oxidized osmocenium Os^+. Indeed, and as shown in Figure 2A, the addition of pyridine drastically modified the cyclic voltammogram of osmocene (**1**). The oxidation wave of **1** became fully irreversible and its peak current intensity doubled in the presence of excess pyridine, suggesting the occurrence of an ECE mechanism.

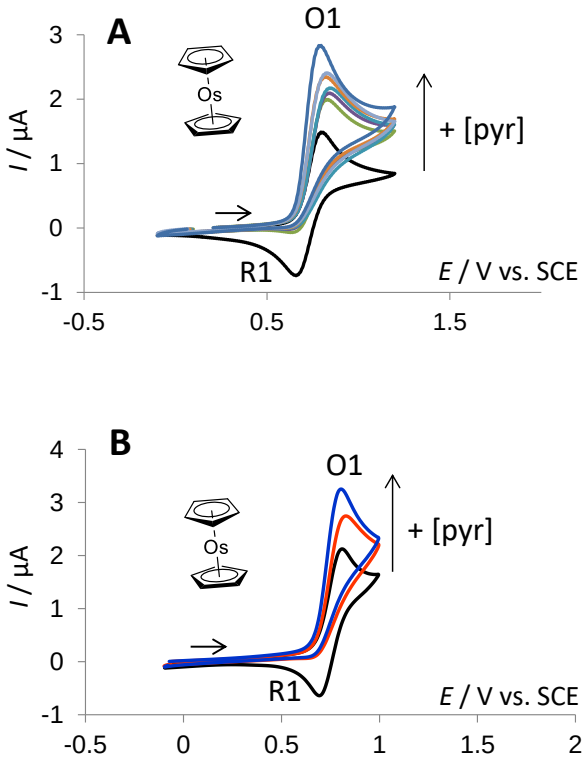

Fig. 2. (A) Cyclic voltammograms of Cp_2Os (**1**, 2 mM), in the absence (black curve) and in the presence of increasing amounts of pyridine (2, 4, 10, 20 and 40 mM, respectively). (B) Cyclic voltammograms of Cp_2Os (2 mM), in the presence (black curve) of lutidine (60 mM) then after addition of pyridine (2 mM, red curve and 4 mM, blue curve). Conditions: studies performed in DCM/[TBA][TFAB] (0.1M); Pt electrode, 0.5 mm in diameter; scan rate 200 mV/s.

A similar behavior was observed for ruthenocene [19] and was interpreted, considering the reactivity of the electrogenerated 17-electron species towards pyridine, to give the corresponding $(Cp_2Os\text{-}Py)^+$ complex, which is immediately oxidized at a similar potential value into the 18-electron dication $(Cp_2Os\text{-}Py)^{2+}$. Accordingly, the susceptibility of $(Cp_2Os)^+$ toward nucleophilic attack can be ascribed to the large ring-ring separation of Cps. Indeed the ring-ring distances for Cp_2M, where M = Fe, Ru, and Os, were reported as being 3.32 [28], 3.68 [29], and 3.71 Å [30], respectively.

Lutidine, sterically hindered and expected to preclude the attack of the metal center, was therefore preferred as the base model (pKa = 6.65 *vs.* 5.22 for pyridine). As shown in Figure 2B (black curve), the cyclic voltammogram of **1** remained fully reversible in the presence of lutidine even used in excess. Under these conditions, and as expected, the addition of low amounts of pyridine was enough to make the cyclic voltammogram irreversible (Figure 2B, red and blue curves).

3.2. Electrochemical behavior of 3 in the absence and the presence of lutidine

3.2.1. In the absence of lutidine

In DCM/[TBA][TFAB] and without any added base, the cyclic voltammogram of **3** exhibited an oxidation wave O3 which was irreversible at low scan rates. Under the same conditions, a fully

reversible oxidation wave was obtained for **2** (E° = 0.71 V) indicating that the irreversibility observed for **3** was related to the presence of the OH group (compare Figures. 3A and 3B).

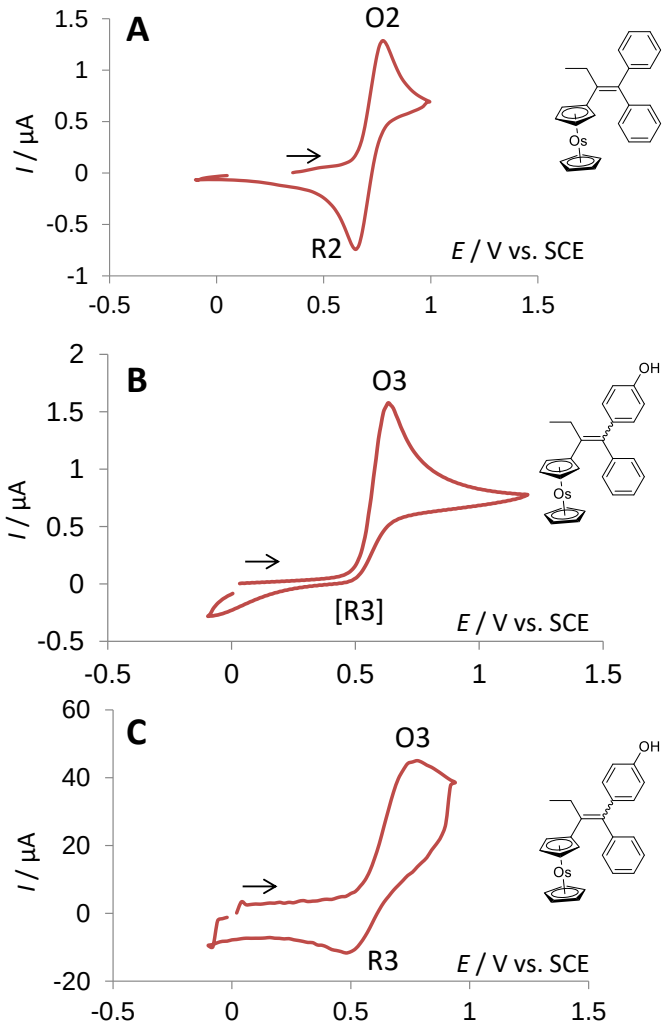

Fig. 3. Cyclic voltammogram of (A) complexes **2** (2 mM) and (B) **3** (2 mM) at 200 mV/s. (C) cyclic voltammogram of complex **3** (2 mM) at 250 V/s. Conditions: studies performed in DCM/[TBA][TFAB] (0.1M); Pt electrode, 0.5 mm in diameter.

This result differs from what was observed for ferrocifens (E° = 0.39 V [16]) and ruthenocifens (E° = 0.76 V [19]) where reversible oxidation waves were obtained in the absence of base [16, 19]. This suggests that the acidity of the phenol group depends on the nature of the metal, the acidity increasing in the order Fe < Ru < Os. By comparison to our previous investigations on iron compounds [15, 16], the phenol on **3** could undergo spontaneous deprotonation after oxidation followed by an intramolecular electron transfer between phenolate and the electrogenerated osmocenium cation through the π-conjugated system.

Interestingly, the oxidation process of **3** was reversible at high scan rate (Figure 3C). Considering that the intramolecular electron transfer between electrogenerated Os^+ and the hydroxyl group OH (not discriminated and referred to as $\mathbf{3}^+$ in Scheme 2) is too fast to be kinetically frozen at 250 V/s [31], it can be assessed that the irreversibility arises from the subsequent deprotonation of the phenol

group (**3**$^{+}$ → **3**$^{\bullet}$ in Scheme 2). Therefore, the oxidation of **3** yields the corresponding phenoxy radical 3$^{\bullet}$, even in the absence of base.

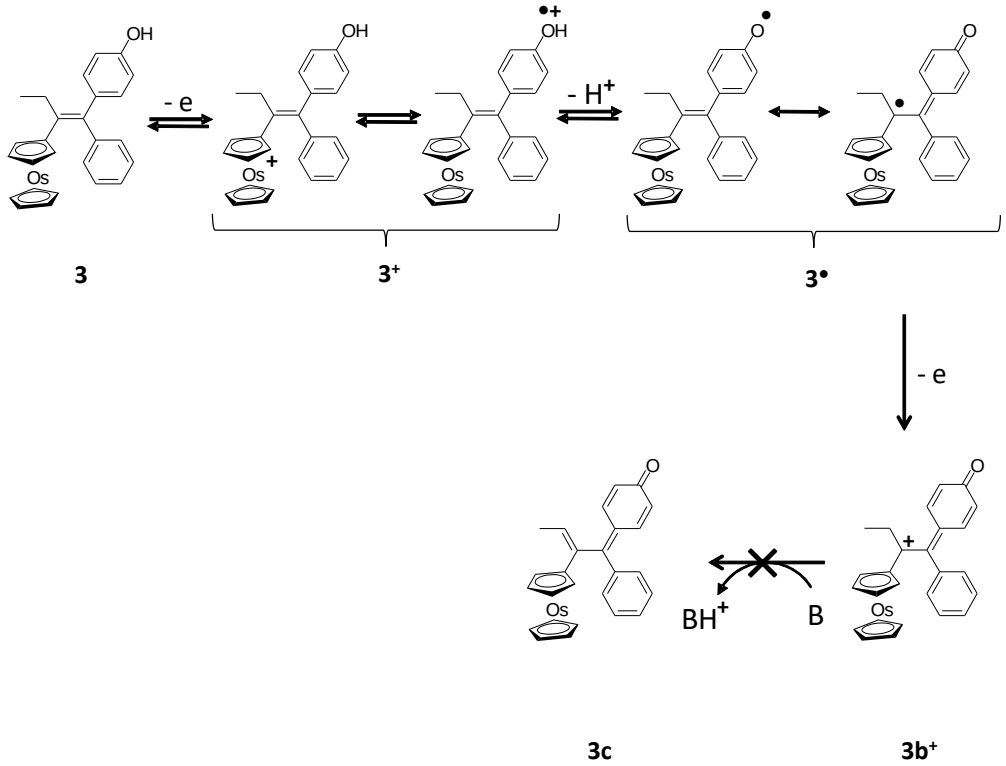

Scheme 2. Detailed oxidation sequence of **3** (Oc-OH) in the absence and the presence of a non-nucleophilic base such as lutidine.

3.2.2. In the presence of lutidine

Upon addition of increasing amounts of 2,6-lutidine, the intensity of the irreversible oxidation wave of **3** increased until reaching twice its initial peak current intensity and shifted towards less positive potential values at 200 mV/s (Figure 4A). These changes were less dramatic at higher scan rate (Figure 4B).

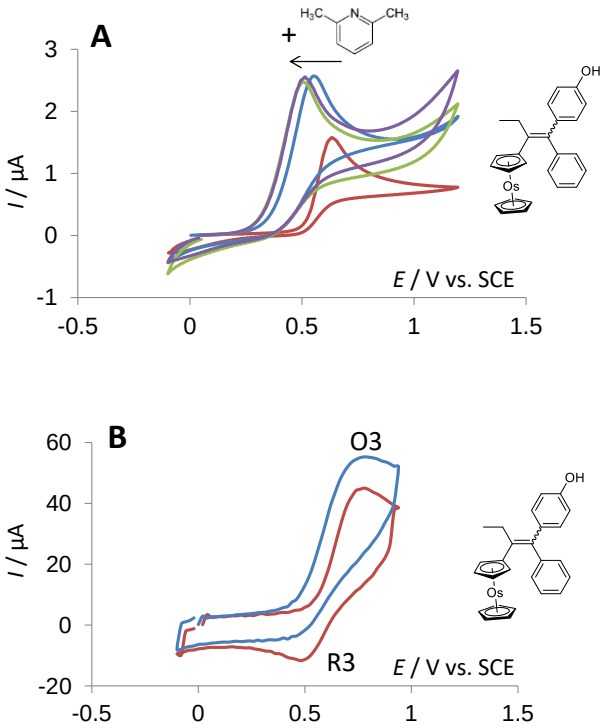

Fig. 4. (A) Cyclic voltammogram of complex **3** (2 mM), at 200 mV/s, in the absence (red curve) and the presence of increasing amounts of lutidine (2, 4, and 20 mM respectively). (B) Cyclic voltammogram of complex **3** (2 mM), at 250 V/s, in the absence (red curve) and the presence of lutidine (2 mM). Conditions: studies performed in DCM/[TBA][TFAB] (0.1M); Pt electrode, 0.5 mm in diameter.

As for ferrocifens [24], the presence of a base apparently allowed a 2-electron oxidation of **3**. However, and contrary to the results reported on ferrocifens, no additional oxidation peak ascribed to a stable quinone methide (**3c** in Scheme 2) was observed.

These results led us to analyze by cyclic voltammetry an authentic sample of quinone methide **3c** prepared by chemical oxidation with Ag_2O. As shown in Figure 5, the cyclic voltammogram of **3c** exhibited an irreversible ill-defined oxidation wave at low scan rate (200 mV/s). Conversely, a well-defined reversible wave was obtained at high scan rate (250 V/s) indicating that the oxidized species generated from **3c** was stable only over few milliseconds.
Furthermore and as already established with the ruthenium derivative, **3c** appeared to be unstable in basic media. As shown in Figure 5, the initial **3c** oxidation wave observed at low scan rate disappeared to the benefit of a new one located at a more positive potential value in the presence of lutidine. As observed with ruthenocifens, this new oxidation wave could be assigned to the oxidation of a cyclic derivative obtained through a base-promoted rearrangement of the **3c** [19].

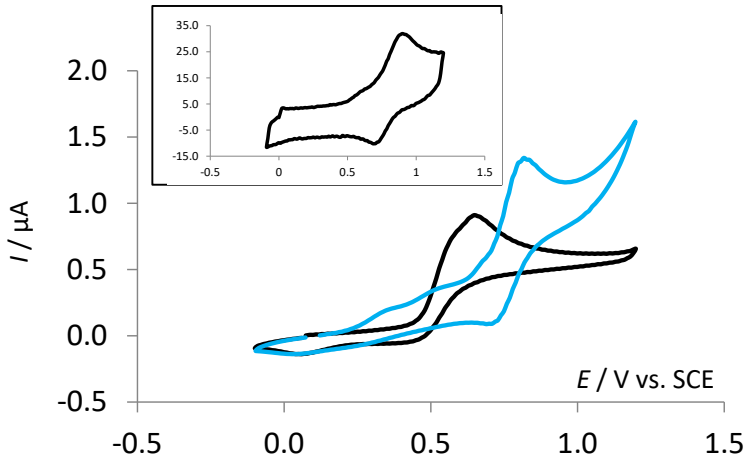

Fig. 5. Cyclic voltammogram of the authentic quinone methide of complex **3** (1.5 mM), in DCM/[TBA][TFAB] (0.1M), at 200 mV/s, in the absence (black curve) and in the presence (blue curve) of lutidine (2 mM). Inset: Cyclic voltammogram of the authentic quinone methide of complex **3** obtained at 250 V/s.

Finally, the electrochemical behavior of **3** revealed a dramatic base dependence: in the absence of lutidine only a monoelectronic oxidation was observed, followed by deprotonation to yield **3**$^{\bullet}$. When lutidine was present, a 2-electron oxidation was observed, which did not give the quinone methide **3c** as the final stable metabolite. This is a striking difference compared to what was observed with ferrocifens (formation of a stable quinone methide) and with ruthenocifens (formation of a transient quinone methide). Accordingly, it was shown that the enzymatic oxidation of **3** did not produce the quinone methide **3c**, but the corresponding carbocation **3b**$^{+}$ (Scheme 2) [21].

Interestingly, it was recently established that osmocenyl-tamoxifen derivatives are prone to target the thioredoxin system [21]. More precisely, *in vitro* assays showed that thioredoxin was inhibited by the carbocation arising from the oxidation of **3**$^{\bullet}$ (**3b**$^{+}$ in Scheme 2). This result is in agreement with the stabilization sequence of carbocations and radicals in the metallocene triad, in the order Fe < Ru < Os, with osmium being the most stabilized [32, 33]. Actually, in ruthenium compounds, the stabilization of the cation analogous to **3b**$^{+}$ results from electron donation of the metal to the Cp ligand - through overlapping of a filled metal *d*-orbital with the LUMO of the Cp ligand - and this overlapping in turn stabilizes the exocyclic carbon [34]. Such a stabilizing effect could help connecting the oxidative behavior of osmociphenols with their cytotoxic properties.

4. Conclusions

We have shown that the general oxidation sequence of osmociphenol **3** differs significantly from that of ruthenociphenol. Firstly, **3** underwent spontaneous deprotonation of its phenol function after oxidation. Secondly, the corresponding quinone methide was not the final and stable complex obtained. This feature can be partially explained by the enhanced stability of the intermediate carbocation **3b**$^{+}$. Finally, despite distinct oxidation pathways, the antiproliferative activities of ruthenocifens and osmocifens are similar and lower than that of ferrocifens. As previously discussed

[22], this could be due to the lower oxidation potential value of ferrocene derivatives which could favor *in vivo* electron transfer [35]. The redox status of these drugs could be investigated *in cellulo* by using the recently published fluorescence modulation of metallocene-based dyads [37].

Acknowledgements

This work was supported by the CNRS (UMRs 8640 and 8232), the Ecole Normale Supérieure, Sorbonne Université and PSL University and by a Research Scholarship under the NTU-ParisTech joint PhD Programme (for H. Z. S. L.). The authors also thank Prof. Dr. Christian Amatore for fruitful discussions.

References

[1] U. Ndagi, N. Mhlongo, M.E. Soliman, Metal complexes in cancer therapy – an update from drug design perspective, Drug Des. Dev. Ther. 11 (2017) 599-616.

[2] P. Zhang, P. J. Sadler, Advances in the design of organometallic anticancer complexes, J. Organomet. Chem. 839 (2017) 5-14.

[3] N.P.E. Barry, P.J. Sadler, Exploration of the medical periodic table: towards new targets, Chem. Commun. 49 (2013) 5106–5131.

[4] G. Gasser, I. Ott, N. Metzler-Nolte, Organometallic Anticancer Compounds, J. Med. Chem. 54 (2011) 3–25.

[5] C.G. Hartinger, N. Metzler-Nolte, P.J. Dyson, Challenges and Opportunities in the Development of Organometallic Anticancer Drugs, Organometallics 31 (2012) 5677–5685.

[6] E.A. Hillard, G. Jaouen, Bioorganometallics: Future Trends in Drug Discovery, Analytical Chemistry, and Catalysis, Organometallics 30 (2011) 20–27.

[7] C. Biot, G. Glorian, L.A. Maciejewski, J.S. Brocard, O. Domarle, G. Blampain, P. Millet, A.J. Georges, H. Abessolo, D. Dive, J. Lebibi, Synthesis and Antimalarial Activity in Vitro and in Vivo of a New Ferrocene-Chloroquine Analogue, J. Med. Chem. 40 (1997) 3715–3718.

[8] G. Jaouen, A. Vessières, S. Top, Ferrocifen type anti cancer drugs, Chem. Soc. Rev. 44 (2015) 8802–8817.

[9] S. Top, J. Tang, A. Vessières, D. Carrez, C. Provot, G. Jaouen, Ferrocenyl hydroxytamoxifen: a prototype for a new range of oestradiol receptor site-directed cytotoxics, Chem. Commun. (1996) 955–956.

[10] S. Top, B. Dauer, J. Vaissermann, G. Jaouen, Facile route to ferrocifen 1-[4-(2-dimethylaminoethoxy)]-1-(phenyl-2-ferrocenyl-but-1-ene), first organometallic analogue of tamoxifen, by the McMurry reaction, J. Organomet. Chem. 541 (1997) 355–361.

[11] Y. Wang, P. Pigeon, S. Top, M.J. McGlinchey, G. Jaouen, Organometallic Antitumor Compounds: Ferrocifens as Precursors to Quinone Methides, Angew. Chem. Int. Ed. 54 (2015) 10230–10233.

[12] Y.G. de Paiva, F. da Rocha Ferreira, T.L. Silva, E. Labbé, O. Buriez, C. Amatore, M. O.F. Goulart, Electrochemically Driven Supramolecular Interaction of Quinones and Ferrocifens: An Example of Redox Activation of Bioactive Compounds, Current Topics in Medicinal Chemistry 15 (2015) 136–162.

[13] J. de Jesús Cázares-Marinero, O. Buriez, E. Labbé, S. Top, C. Amatore, G. Jaouen, Synthesis, Characterization, and Antiproliferative Activities of Novel Ferrocenophanic Suberamides against Human Triple-Negative MDA-MB-231 and Hormone-Dependent MCF-7 Breast Cancer Cells, Organometallics 32 (2013) 5926–5934.

[14] J. de Jesús Cázares-Marinero, E. Labbé, S. Top, O. Buriez, C. Amatore, G. Jaouen, The effect of protic electron donor aromatic substituents on ferrocenic and [3] ferrocenophanic anilines and anilides: Some aspects of structure-activity relationship studies on organometallic compounds with strong antiproliferative effects, J. Organomet. Chem. 744 (2013) 92– 100.

[15] Y.L.K. Tan, P. Pigeon, S. Top, E. Labbé, O. Buriez, E.A. Hillard, A. Vessières, C. Amatore, W.K. Leong, G. Jaouen, Ferrocenyl catechols: synthesis, oxidation chemistry and anti-proliferative effects on MDA-MB-231 breast cancer cells, Dalton Transactions 41 (2012) 7537–7549.

[16] P. Messina, E. Labbé, O. Buriez, E.A. Hillard, A. Vessières, D. Hamels, S. Top, G. Jaouen, Y.M. Frapart, D. Mansuy, C. Amatore, Deciphering the Activation Sequence of Ferrociphenol Anticancer Drug Candidates, Chem. Eur. J. 18 (2012) 6581–6587.

[17] P. Pigeon, S. Top, A. Vessières, M. Huché, E.A. Hillard, E. Salomon, G. Jaouen, Selective Estrogen Receptor Modulators in the Ruthenocene Series. Synthesis and Biological Behavior, J. Med. Chem. 48 (2005) 2814–2821.

[18] E.A. Hillard, A. Vessières, S. Top, P. Pigeon, K. Kowalski, M. Huché, G. Jaouen, Organometallic diphenols: The importance of the organometallic moiety on the expression of a cytotoxic effect on breast cancer cells, J. Organomet. Chem. 692 (2007) 1315–1326.

[19] H.Z.S. Lee, O. Buriez, E. Labbé, S. Top, P. Pigeon, G. Jaouen, C. Amatore, W.K. Leong, Oxidative Sequence of a Ruthenocene-Based Anticancer Drug Candidate in a Basic Environment, Organometallics 33 (2014) 4940–4946.

[20] H.Z.S. Lee, O. Buriez, F. Chau, E. Labbé, R. Ganguly, C. Amatore, G. Jaouen, A. Vessières, W.K. Leong, S. Top, Synthesis, Characterization, and Biological Properties of Osmium-Based Tamoxifen Derivatives – Comparison with Their Homologues in the Iron and Ruthenium Series, Eur. J. Inorg. Chem. 25 (2015) 4217–4226.

[21] V. Scalon, S. Top, H.Z.S. Lee, A. Citta, A. Folda, A. Bindoli, W.K. Leong, M. Salmain, A. Vessières, G. Jaouen, M.P. Rigobello, Osmocenyl-tamoxifen derivatives target the thioredoxin system leading to a redox imbalance in Jurkat cells, J. Inorg. Biochem. 160 (2016) 296-304.

[22] V. Scalon, M. Salmain, A. Folda, S. Top, P. Pigeon, H.Z.S. Lee, G. Jaouen, A. Bindoli, A. Vessières, M.P. Rigobello, Tamoxifen-like metallocifens target the thioredoxin system determining mitochondrial impairment leading to apoptosis in Jurkat cells, Metallomics 9 (2017) 949-959.

[23] F. Chau, C. Amatore, E. Labbé, O. Buriez, Revisiting the Complex Osmocene Electro-Oxidation Mechanism, Electrochim. Acta 212 (2016) 973-978.

[24] C. Amatore, E. Labbé, O. Buriez, Molecular electrochemistry: A central method to understand the metabolic activation of therapeutic agents. The example of metallocifen anti-cancer drug candidates, Curr. Opin. Electrochem. 2 (2017) 7-12.

[25] R.J. LeSuer, C. Buttolph, W.E. Geiger, Comparison of the Conductivity Properties of the Tetrabutylammonium Salt of Tetrakis(pentafluorophenyl)borate Anion with Those of Traditional Supporting Electrolyte Anions in Nonaqueous Solvents, Anal. Chem. 76 (2004) 6395-6401.

[26] S. Top, A. Vessières, G. Leclercq, J. Quivy, J. Tang, J. Vaissermann, M. Huché, G. Jaouen, Synthesis, Biochemical Properties and Molecular Modelling Studies of Organometallic Specific Estrogen Receptor Modulators (SERMs), the Ferrocifens and Hydroxyferrocifens: Evidence for an Antiproliferative Effect of Hydroxyferrocifens on both Hormone-Dependent and Hormone-Independent Breast Cancer Cell Lines, Chem. Eur. J. 9 (2003) 5223-5236.

[27] G. Jaouen, S. Top, A. Vessières, G. Leclercq, J. Quivy, L. Jin, A. Croisy, The First Organometallic Antioestrogens and Their Antiproliferative Effects, C. R. Acad. Sci. Ser. IIc : Chim 3 (2000) 89-93.

[28] J. D. Dunitz, L.E. Orgel, A. Rich, The crystal structure of ferrocene, Acta Cryst. 9 (1956), 373-375

[29] D.C. Hargrove, D.H. Templeton, The crystal structure of ruthenocene, Acta Cryst. 12 (1959) 28-32.

[30] V.F. Jellinek, Die Struktur des Osmocens, Naturforsch. B 14b (1959) 737-738.

[31] C Amatore, S. Gazard, E. Maisonhaute, C. Pebay, B. Schöllhorn, J.-L. Syssa-Magalé, J. Wadhawan, Ferrocenyl oligo(phenylene-vinylene) thiols for the construction of self-assembled monolayers, Eur. J. Inorg. Chem. (2007) 4035–4042

[32] M.I. Rybinskaya, A.Z. Kreindlin, S.S. Fadeeva, On the problem of stabilization of alpha-carbocationic centers in metallocene series – related interconversions of permethylated alpha-metallocenylcarbocations and metallocenium cation-radicals of the iron sub-group, J. Organomet. Chem. 358 (1988) 363–374.

[33] M.I. Rybinskaya, A.Z. Kreindlin, Y.T. Struchkov, A.I. Yanovsky, On the problem of the stabilization of alpha-metallocenylcarbocation - synthesis, properties and crystal structure of $[C_5Me_5OsC_5Me_4CH_2^+]BPh_4^-.CH_2Cl_2$. J. Organomet. Chem. 359 (1989) 233–243.

[34] N.J. Long, Metallocene: An introduction to sandwich complexes, Blackwell Science, London, 1998, pp 129-132.

[35] P. Kovacic, Unifying mechanism for anticancer agents involving electron transfer and oxidative stress: Clinical implications. Med. Hypotheses. 69 (2007) 510-516.

[36] A. Citta, A. Folda, A. Bindoli, P. Pascal Pigeon, S. Top, A. Vessières, M. Salmain, G. Jaouen, M. P. Rigobello, Evidence for Targeting Thioredoxin Reductases with Ferrocenyl Quinone Methides. A Possible Molecular Basis for the Antiproliferative Effect of Hydroxyferrocifens on Cancer Cells. J. Med. Chem. 57 (2014) 8849-8859.

[37] M. Čížková, L. Cattiaux, J. Pandard, M. Guille-Collignon, F. Lemaître, J. Delacotte, J.-M. Mallet, E. Labbé, O. Buriez. Redox switchable rhodamine-ferrocene dyad: Exploring imaging possibilities in cells Electrochem. Commun. 97 (2018) 46–50.